DOI: 10.13009/EUCASS2023-036
Aerospace Europe Conference 2023 – 10TH EUCASS – 9TH CEAS

Development of an injector sizing tool for a 4kN LOX/Ethanol student-built liquid rocket engine

Rodriguez Castro Gines ⋆ *Aubry Raphaël*⋆ *Parisi Ploumpi Angeliki*⋆†
⋆*ISAE-Supaéro*
Toulouse, France

Abstract

The objective of this work is to develop a sizing tool for impinging and coaxial-type injectors. The tool is built on a database of experimental and theoretical correlations available in the literature for the design of liquid rocket engine injectors. They relate the injector element geometries and propellant properties to the injection pressure losses, liquid droplet size and mixing performance. Doublet impinging, swirl coaxial and shear coaxial element geometries were sized using the tool and presented with their expected respective performances. It is the aim of this work to be a building block for the design of injectors within the PERSEUS project.

1. Introduction and Context

1.1 PERSEUS Student Project & the MINERVA engine

PERSEUS (Projet Étudiant de Recherche Spatiale Européen Universitaire et Scientifique) is a student rocketry initiative with over 30 technical universities working together on the development, manufacturing and testing of sounding rockets. Led by CNES, the French Space Agency, PERSEUS introduces students to engineering challenges by giving them an opportunity to develop viable solutions with an emphasis on building a usable product.

The Perseus sounding rocket, Astreos 1, is powered by the bi-propellant MINERVA MLE5K-S1a rocket engine running on Liquid Oxygen and Ethanol. This engine has been in testing with ArianeGroup and both cold flow and hot fire tests have been conducted. Presently, the engine's injection system consists of seven F-O-F triplet elements designed to achieve the target performance summarized in Table 1. Higher than expected pressure losses have been measured however, decreasing the pressure in the chamber. The time history of the mixture ratio has also shown that the triplet impinging injectors cannot provide the desired uniformity to reach the target engine performance. It is therefore necessary to build a better understanding of injector design to improve this key component of the propulsion system.

Property	Value
Propellants	LOX-Ethanol
Chamber Pressure	20 bar
Mixture Ratio	1.4
Vacuum Thrust	5 kN
Vacuum Specific Impulse	295 s
Mass Flow Rate	2.1 kg/s
Combustion Temperature	3100 K
Combustion Time	20 s
Min. Combustion Efficiency	0.95

Table 1: MLE5K-S1a engine overview and target performance

1.2 Rationale for an injector design tool

The injector of a liquid propellant rocket engine (LPRE) is known to be the component which most influences the success or failure of the thrust chamber combustion. This has been demonstrated with the MINERVA as mentioned above,

DOI: 10.13009/EUCASS2023-036

and with all LPREs. The most important parameters characterizing injector performance are mixing, atomization and pressure drop, cooling and combustion instabilities. These differ from one injector design to another and will be treated in detail under each injector section.

Mixing is a key factor, as it allows the combustion to take place. Mixing performance is dependent on the mass ratio, the choice in spatial distribution of injector orifices across the plate and on the atomization of liquid reactants.[23]

Instabilities are vibrations formed during combustion that can be detrimental to the performance of the engine, especially when coupled with other resonant frequencies. They can be divided into high and low-frequency instabilities: Chug instabilities are low frequency, between 50 to 250Hz, caused by the coupling of the feed system with the combustion chamber. Buzz, Acoustic and Hybrid are High- frequency instabilities between 100 and 900Hz, among others. These instabilities are normally treated with suppression devices, dams or resonators. However, in the case of small-scale engines, the resonance frequencies are so high that hardly any coupling is found.[41]

Cooling or thermal considerations are key for the proper functioning of the injection system. The injector has to be prepared to bear the high temperatures of the combustion chamber and the thrust chamber has to be designed by keeping in mind heat spots at the walls. A general rule was found which is that, if no active cooling is used on the engine it is better to opt for fuel-rich propellant mixtures near the chamber walls. A trade-off therefore has to be found by the engineer, between cooling considerations and mixture uniformity, which both affect performance.[23,41]

Pressure loss refers to the difference in total pressure between the inlet of the injector and the combustion chamber. A lower pressure loss leads to lower tank pressures or less powerful turbopumps, hence an overall lower system mass. Pressure losses can be related to the *Discharge Coefficient* C_d. This dimensionless parameter, shown in Equation 1 relates the design mass flow rate through the injector to the pressure loss, geometry and liquid density.

$$C_d = \frac{Q\rho}{A\sqrt{2\rho\Delta p}} = \frac{\dot{m}}{A\sqrt{2\rho\Delta p}} = \frac{V_j}{\sqrt{2\Delta p/\rho}} \tag{1}$$

2. Injector system pre-sizing

The injector design is always constrained by the specifications of the mission. The target thrust level is directly related to the mass flow, and the choice of propellant then fixes an optimal oxidizer/fuel mixing ratio. The necessary propellant droplet size for complete evaporation and combustion, is an important guiding criterion for injector pre-sizing.

A method reviewed Kuo[26] was used to estimate droplet evaporation time and distance in a quiescent atmosphere for LOx and Ethanol. The method assumes that the droplet surface temperature does not vary in time and the droplets spherically diffuse their mass. Droplet evaporation can be described according to the d^2-evaporation law presented below.

$$D^2 = D_o^2 - \beta_v \cdot t \tag{2}$$

where, D_o is the initial droplet diameter after atomization, t is the time after atomization and β_v is the mass transfer coefficient. The mass transfer coefficient β_v is defined according to the Spalding mass transfer number B_M in Equation 3,

$$\beta_v = \frac{8\rho_s\alpha_s}{\rho_l} ln(1 + B_M) \tag{3}$$

where, ρ_s and ρ_l are taken as the combustion gas density and the droplet liquid density at injection respectively, while α_s is the thermal diffusivity of combustion gases defined as $\alpha_s = (k/\rho C_p)_s$.[26]

Making the assumption that equal mass and thermal diffusivity occur across the droplet boundary with chamber gases, B_M can be computed for the case of an evaporating droplet using Equation 4,

$$B_M = \frac{C_p(T_\infty - T_s)}{\Delta h_v} \tag{4}$$

where T_∞ is the temperature in the far field, so here the combustion chamber total temperature.

Variables with subscript s would normally refer to droplet surface conditions however such detail would require further attention as to the heat transfer modeling of droplets, which falls outside the scope of this work. T_s was fixed at the propellant vaporization temperature at chamber pressure. The NASA Chemical Equilibrium with Applications code[16] was used to obtain thermodynamic variables of combusting gases. The selected approach is a simplification from the actual engine conditions, in which LOx droplets are evaporating with the contribution of aerodynamic effects and Ethanol droplets are evaporating and burning. An inherent margin of safety on the maximum droplet size is therefore secured with this method.

DOI: 10.13009/EUCASS2023-036

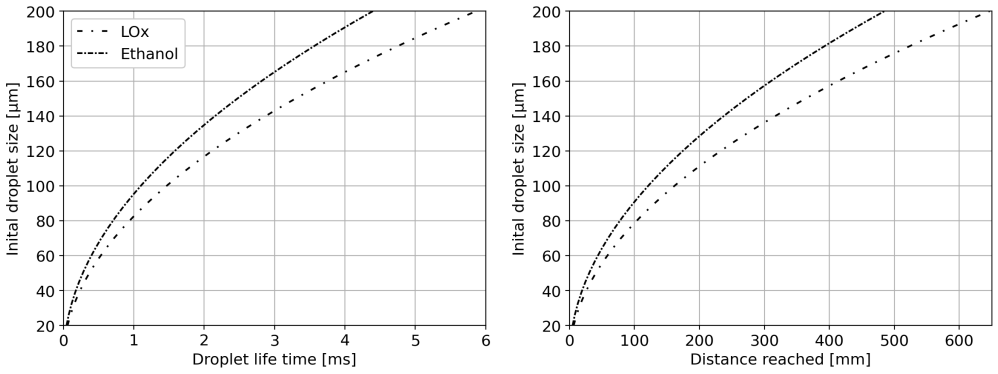

Figure 1: (**Left**) Estimated life time and (**Right**) corresponding distance of droplet until evaporation for chamber conditions of the MINERVA

Taking $D = 0$ in Equation 2 gives the droplet evaporation time for a given initial droplet size, and assuming chamber gas velocities of Mach=0.1 the distance life can also be obtained, as depicted in Figure 1. With a chamber of approximately 0.3cm for the MINERVA, the required droplet sizes of Ethanol and Liquid Oxygen are 160 μm and 140 μm respectively. From Figure 1 it is observed that given an equal initial droplet size, the Liquid Oxygen droplet will take longer to evaporate.

.

3. Impinging Injectors

Impinging injectors have demonstrated their reliability and good performance for decades. Examples include US projects like the Gemini first stage running on NTO/A-50, the Rocketdyne F1 of the Apollo program using LOX/RP-1, the European Viking V powering the Ariane or Chinese Long March 3 & 4.[2] All of these engines and many others used like-doublets (LD) impinging injectors, which consist in pairs of intersecting fuel-fuel and oxidizer-oxidizer jets. Other types include the unlike-doublet (UD) with impinging fuel-oxidizer jets, and triplet injectors which have a central jet intersected by two jets. The latter can be either designed as an O-F-O or an F-O-F. Finally there can also be quadlet impinging jets, where doublet pairs impinge as a four jet intersection.

3.1 Geometry

The geometry on impinging injectors is defined by the orifice diameter d_o, orifice length L_o, impingement angle 2θ and liquid jet length to the point of impingement L_j, as depicted in Figure 2 and 3. Each type of impinging injector provides different levels of performance and can be qualitatively assessed in the following ways. LD elements demonstrate stable combustion while providing moderate mixing performance levels.[23] This type has the advantage of being easy to manifold across an injection assembly and provides a distributed combustion volume across the chamber. In UD elements, rapid mixing is promoted by direct impingement of oxidizer and fuel, which quickens the combustion. Both UD and LD schemas follow the same architecture as in Figure 2. With triplet injectors, the Fuel-Oxidizer-Fuel type tends to produce better atomization of the fuel, while the O-F-O improves mixing for thrust chambers with higher oxidizer momentum ratios. With a mixture ratio of 1.4 in the MINERVA engine, the F-O-F is a good choice of unlike impinging element. LD elements should however reduce the thermal gradients of unlike impinging injectors,[23] which is a sensible choice for the ablative-cooled chamber of the MINERVA.

3.2 Mixing

As pointed out by Inoue et al.,[22] the Rupe and Elverum-Morey parameters have essentially been the main guiding tools for unlike impinging injectors.

Mixing Criteria. Rupe put forward the hypothesis that optimal unlike-doublet jet mixing occurred with equal jet momentum and jet diameters. This mixing criterion has been widely used and is a reference in UD element design. The Elverum-Morey parameter was an extension of the Rupe criterion to triplet elements, however Ferrenberg et al.[12] tested its effectiveness with water tests and showed that it could not predict optimal triplet mixing. The same authors then proposed their own correlation for estimating propellant mixing in triplet elements, considering orifice geometry,

DOI: 10.13009/EUCASS2023-036

impingement angle, liquid densities and jet velocities. Recently the work of Rupe was successfully extended by Inoue et al.,[22] who demonstrated that the ratio of oxidizer to fuel spray width should be equal for best mixing. Their work was tested and validated for UD and triplet elements, with ranges of oxidizer-to-fuel ratios of density and orifice diameters of 1-1.3 and 1.2-1.8 respectively.

In UD elements, the relative distance at which individual pairs of oxidizer-oxidizer and fuel-fuel pairs break-up directly impacts local mixture ratios within the chamber.[23] Such efforts to quantify the distance of liquid sheet and ligament break-up after impingement has been carried out by a number of authors.[4,29,37,42] Most recently, Sweeney and Frederick[42] showed that sheet break-up lengths reached a peak at a transition Weber number solely dependent on impingement angle, then steadily decreased with increasing Weber.

Relation between mixing and discharge losses. Sharp edges at the entrance cause flow contraction by means of a vena contracta, which can cause liquid cavitation if local static pressure in the contraction region is lower than propellant vapour pressure. Cavitation leads to bubble formation which disturbs the internal flow, resulting in poor quality exit jet and subsequently, poor mixing.[35] This effect would be prominent in cryogenic propellant injection, however curved edge inlets should negate this problem.[2]

Jet misalignement. Misaligned jets is the main problematic in the manufacturing of impinging jets. Small deviation from the jet plane cause significantly lower mixing efficiency and therefore combustion efficiency. Subedi et al.[39] demonstrated by water testing that the ratio of the lateral offset distance to jet diameter for LD elements should remain below 30%, otherwise impacting spray angle and jet break-up lengths.

Engine throttling. Throttling was also considered as it impacts the transient behaviour of the engine. Ferrenberg et al.[12] demonstrated that a reduction to 67% of the baseline mass flow rate for doublet elements, led to a maximum loss in mixing efficiency of 4%. Such result indicates that start-up transients and thrust varying flight sequences have a relatively small effect on engines with impinging injectors.

3.3 Atomization

A number of correlations are available for the droplet size estimation of like-doublet injectors and have been reviewed 2 with corresponding ranges of validity, however UD element literature focuses mostly on mixing studies.

Element geometry. As a general rule, smaller orifice diameters will provide better atomization, which has been predicted since early investigations[4] to more recent ones.[42] A value between 0.8mm and 2.5mm is advised to avoid clogging of the orifice and maintain good atomization. Orifice length has little impact on atomization as long as the ratio of L_o/d_o can be kept above 1.5 to allow for contracted flow to reattach itself to the wall in sharp orifices.[2] The upper limit of the ratio then depends on the allowable pressure loss.

Injection conditions. There seems to be no specific rule for injection velocities through impinging injectors but the literature range could be estimated to be 10-40 m/s, depending on required mass flow, propellants used and element dimensions. High injection velocities lead to finer droplets, but also higher pressure drop, as depicted in Figure 4 (Left), where the increasing pressure loss depicts this increasing jet velocity. However, Lai 2005 proposed that above a jet velocity of 30 m/s, the SMD reached an asymptotically steady value, regardless of liquid viscosity and surface tension.[27]

Authors have shown that ambient gas density is an important component of liquid jet atomization, decreasing droplet sizes with denser chamber gases.[4,29,37] Bailardi[1] studied a wide range of liquids, noting that with increased chamber pressure, break-up lengths shortened, leading to earlier atomization of the liquid sheet. He also showed that the spatial density of liquid droplets within the spray increased with increasing chamber pressures, promoting droplet spread and hence propellant mixing. Zajac[46] and George[14] brought to light the strong influence of chamber gas velocities on the atomization of like-doublets, predicting a division by a factor of 3 in droplet size when relative liquid-

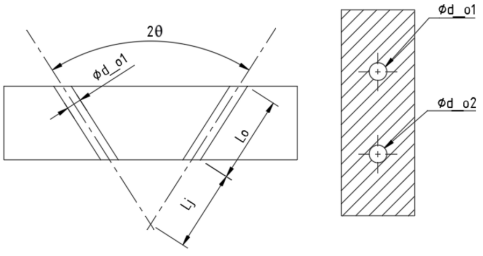

Figure 2: Doublet impinging injector

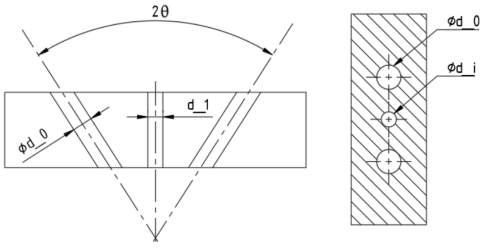

Figure 3: Triplet impinging injector

DOI: 10.13009/EUCASS2023-036

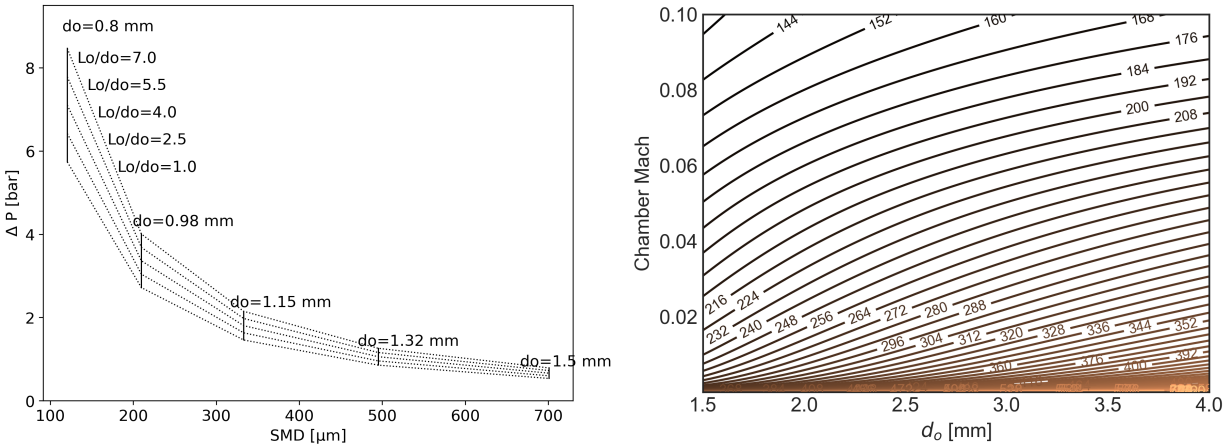

Figure 4: (**Left**) *Sauter Mean Diameter* estimation for injecting Ethanol at room temperature against the pressure drop for a sharp orifice of varying geometry. SMD computed from the correlation of Hautman 1991[17] in Equation (5) and ΔP computed using the correlation of Bazarov et al.[2] in Eq. 6. (**Right**) *Mass Median Diameter* estimation of a LD element with respect to orifice diameter and chamber mach number using the correlation of Zajac 1973,[46] assuming a chamber speed of sound of 1000m/s and a jet velocity of 50m/s (isolines = MMD)

gas velocities, of up to 4 were tested (relative velocity measured as $(V_{gas} - V_L)/V_L$). The right hand-side of Figure 4 impact of the chamber Mach number and orifice diameter on the Mass Median Diameter (MMD) of liquid droplets, plotted within the experimental ranges of the correlation. The MMD is of interest to injector designers because it indicates that 50% of the liquid droplets have larger diameters than the value obtained. Taking the best case scenario predicted for Ethanol of 136-144 μm, the estimation is below the required droplet size.

$$SMD = 1.3 \times 10^7 (\rho_L V_j^2)^{-0.7} \sigma^{0.6} \rho_g^{-0.09} \tag{5}$$

3.4 Combustion instabilities of impinging

As two or more liquid jets impinge on each other, they form a liquid sheet, followed by a break-up of the sheet, continued by periodic ligament formations and successive atomization of the smallest ligaments into droplets.[28] Initially with the work of Dombrowski and Hooper[4] and later continued by Ryan,[37] was shown that there could be a link between the periodicity of liquid ligament breaking and flame instabilities within a LPRE combustion chambers.

3.5 Discharge coefficient and pressure loss

It is interesting to see that the methods for estimating the coefficient of discharge in an impinging type element and the corresponding losses, vary to a somewhat important degree between references. Classical textbook approaches[41] will advise the use of fixed coefficient of discharge depending uniquely on orifice aspect ratio and the binary choice of either round or sharp entrances. Others define pressure losses as being mostly due to viscous effects, with the friction factor being estimated according to pipe flow losses. This was the approach of Sweeney and Frederick.[42] Efficient pressure loss estimation will however necessitate prediction of manufacturing effects, propellant cavitation and naturally the precise element geometry.[2,15,35]

Relating C_d and ΔP_{inj} selection. The discharge coefficient and pressure loss are inter-related as described by Equation 1. In pre-sizing, one variable is an input for estimating the other, however generally with impinging design the designer will want to predict the discharge coefficient based on available literature and later perform water tests to validate the injector performance. Nonetheless there is a clear trade-off analysis to perform regarding the necessary pressure loss to be assigned to an injector plate and the maximum propulsion system and feed-system weight. A pressure loss of 15-25% of chamber pressure to prevent gases from circulating back through the injector is usually advised for impinging injectors.[41]

Estimating C_d. Friant 1954 proposed correlations based mostly on geometrical parameters, also considering the direction of hole drilling with respect to the plate. Multiple cases were considered with their respective correlating curves for C_d; drilling of inward uniform burr and re-entry burr, clean sharp edge and rounded edge. A burr refers to the yielded metal causing an extruding edge upon drilling or other machining processes. Sharp edged orifices lead

DOI: 10.13009/EUCASS2023-036

Reference	D	Experimental conditions
Dombrowski and Hooper 1964[4]	d_{32}	Water, $7.3 \leq V_j \leq 19.5$ m/s, $50° \leq \theta \leq 140°$
Ingebo 1958[21]	d_{30}	n-heptane, 203 mm from injector, $0.74 \leq d_j \leq 2.26$ mm, $9.15 \leq V_j \leq 30.5$ m/s, $19.8 \leq V_g \leq 91.4$ m/s, $\mu_L = 3.6 \cdot 10^{-4}$ Pa-s, $\rho_L = 680\ kg/m^3$, $\sigma = 20$ mN/m, $\theta = 90°$
Dickerson et al. 1968[3]	$\overline{d}$	Hot wax, $0.66 \leq d_j \leq 2.06$ mm, $15.5 \leq V_j \leq 45.3$ m/s, $V_g = 0$, $\theta = 60°$, $\mu_{wax} = 3$ mPa-s, $\rho_{wax} = 764\ kg/m^3$, $\sigma_{wax} = 17$ mN/m
Zajac 1971[45]	$\overline{d}$	Hot wax, $1.52 \leq d_j \leq 2.06$ mm, $9.14 \leq V_j \leq 67.0$ m/s, $45° \leq \theta \leq 90°$, same wax properties as above
Zajac 1973[46]	$\overline{d}$	Hot wax injected into warm flowing nitrogen, $23.2 \leq V_j \leq 76.2$ m/s, $\theta = 60°$, $V_g \leq 305$ m/s, $\rho_g = 1\ kg/m^3$, $L_{cc} > 5$ cm, same wax properties as above
George 1973[14]	d_{30}	N_2H_4 drops burning in N_2H_4 and water injected in N_2, $1.5 \leq d_j \leq 2.44$ mm, $18.6 \leq V_j \leq 38.7$ m/s, $75.6 \leq V_g \leq 114$ m/s, $\theta = 60°$
Lourme 1986[31]	d_{10}	Water tests followed by validations for N_2O and UDMH , $d_j \leq 3$ mm, $20 \leq V_j \leq 40$ m/s,$\rho_g \leq 6.5\ kg/m^3$, $0.33 \leq \mu_L \leq 5.7$ mPa-s,$\sigma \leq 25$ mN/m, $\theta = 90°$
Hautman 1991[17]	d_{32}, $\overline{d}$	Water, Freon 113 and Jet A, $0.0453 \leq \dot{m} \leq 0.307$ kg/s, $1.7 \leq 10^4 Re \leq 8.4$, $1.3 \leq$ momentum flux $\leq 5.7\ 10^4\ kg/m - s^2$, $1 \leq \rho_g \leq 30\ kg/m^3$, $T_{cc} = 926.85K$
Ryan et al. 1995[37]	d_{10}	$5 \leq V_j \leq 20$ m/s, $35 \leq l_o/d_o \leq 80$, $18 \leq l_j/d_o \leq 40$, $40° \leq \theta \leq 80°$, $Re > 2.3 \times 10^3$
Lim et al. 2004[29]	d_{10}	Water injected into pressurized N_2, valid for $0 \leq (\rho_g/\rho_L)^{-1/6} We_j^{-1/3} \leq 0.4$, $\theta = 90°$
Sweeney and Frederick 2016 Sweeney and Frederick 2016[42]	d_{10}	Water, break-up length/impingement length ≥ 1, $30° \leq \theta \leq 90°$

Table 2: *Like-doublet* impinging injector correlations for droplet size estimation

to lower C_d, and increasing the roundness at the entrance increases the coefficient. At best, a sharp orifice with no burrs will provide a C_d of 0.8, while one with an important ratio of edge curvature to orifice diameter will move the coefficient up to nearly 1. One loss is however that seems to be only implicitly considered in their work is the frictional loss variation with orifice aspect ratio variation.

A method proposed by Bazarov et al.[2] was found to be the most complete one, as it allows the designer to consider entrance effects due to the Reynolds, flow contraction-expansion loss, and frictional losses according to the orifice aspect ratio. The contraction-expansion loss ζ_{cont}(edge) refers to the energy lossed to vortices upon expansion after the sudden flow contraction due to sharp or slightly non-smooth inlet edge. The entrance contribution ζ_{ent} term was shown to decrease with increasing Reynolds, and to disappear above $Re = 10^5$, which is easily the case for LPREs in steady engine conditions. Equation 6 describes the computation of the pressure loss according to this method, plotted in 4. The discharge coefficient correlation by Friant 1954[13] was compared to that of Bazarov for injecting Ethanol and was found to overestimate losses by over 100%.

$$\Delta p_{inj} = \zeta_{total} V_j^2 \rho_L / 2 = \left[\zeta_{ent}(Re) + \zeta_{cont}(\text{edge}) + \zeta_{fr}(Re,\ L_o/d_o)\right] V_j^2 \rho_L / 2 \tag{6}$$

In the method proposed by Nurick,[35] he estimated the discharge coefficient in the case of sharp and round edged orifices. In the former, once flow is established and cavitation occurs, C_d is found to be linearly proportional to the flow contraction ratio when in the vena contracta. Then, knowing the total pressure in the plenum P_1 (the large volume upstream of the element), the ambient back pressure or chamber pressure in the case of an engine P_c, and the liquid vapour pressure at the tank temperature, an expected discharge coefficient can be found. This approach is however more of an experimental one, as it is difficult to estimate the achieved pressure balances on paper or using a coding script. For rounded edges, cavitation was shown to be prevented for edge roundness radius of curvature ratio with orifice diameters above 0.14.

Impinging injector sizing: From the above considerations, a like-doublet impinging injector sizing has been proposed for the LOX/Ethanol combination, using 2 pairs of elements for each propellant. Mixing has been taken into

DOI: 10.13009/EUCASS2023-036

consideration by computing break-up lengths of the two jets using recently published works of Sweeney 2016.[42] To obtain the droplet size previously defined of 140 μm and 160 μm for the LOx and Ethanol, the correlation of Hautman 1991 indicates that jet velocities must be 15 m/s and 60 m/s respectively. Using Equation 6 estimated pressure losses are 0.47 bar and 5.21 bar for the LOx and Ethanol elements respectively. Although the pressure losses and break-up lengths are good, a problem arises, which is that following the predictions of Lai 2005,[27] fuel droplets would actually be within 45 μm at such velocities, which would vaporize the fuel before the liquid oxygen, hence leading to improper mixing. Further, the designer should account for the considerable sensitivity of this injector to manufacturing tolerances, limiting misaligned jets. The mixing constraint would seem to disappear with the unlike impinging jets, however not solving the latter and the pressure loss problematic. In fact, as shown in Figure 4, to reach droplet sizes below 200 μm for Ethanol requires an important pressure loss increment.

	ΔP (bar)	**Break-up length (mm)**	**d_o (mm)**	**2θ °**	**L_o/d_o**
LOX	0.47	9.2	1.35	60	4
Ethanol	5.21	6.7	0.8	60	4

Table 3: Like doublet geometrical configuration with short relative break-up length, presented with corresponding pressure loss in LOX and Ethanol LD eleme nts

4. Swirl Coaxial

The swirl injector encompasses any injector which uses centrifugal flow as its energy-converting method for atomizing the propellants. Methods used to provide the tangential velocity component include tangential inlets, axial helical slots or a combination of both.[28] One of the most recent applications is the RL-10 engine from the "Centaur" upper stage, using LOX and LH2.[33]

Another relevant application is the injector in the RD-170 engine[9] used as a booster for the Soviet "Energuia" rocket. This engine's main injector plate was reused in the RD-180[10] engine and fired in the Atlas V boosters. These would run LOX and Kerosene, turning the oxygen gaseous before injection.

However, all these are used for high-thrust applications, and completely different geometries were found for applications closer to the Minerva. A NASA viability study for the Orbital Manoeuvring System (OMS) of the Space Shuttle Orbiter (SSO)[8] suggest the design from Figure 5. This design would use Ethanol with LOX with a thrust range between 3500-6000 lbf matching the Minerva engine's requirements. This injector type was also found on the proposal from DLR for a Small Satellite Launch Vehicle (SSLV) for the European project SMILE.[19] Both of these injectors are versions of the Russian heritage swirl injector, which was heavily studied and used in the first versions of the Soyuz rocket,[40] implemented in the RD-107 engine. This design was said to be the ideal thanks to its reliability against machining imperfections guaranteeing good performance.[5]

4.1 Geometrical considerations

Focusing on the injector type from the RD-107,[40] the injection element has a very particular geometry to swirl the flow to achieve enhanced atomization. Its parts are described in Figure 5. It consists of two "Simplex" swirls that are embedded one inside another.

The "Simplex" injector, which can be seen in Figure 6, has been heavily studied, being very efficient for oil-air combustion in turbines.[24] The fuel is steady at a pressurized dome before injection through hole "Dp". The eccentricity in the swirl chamber "Ds", allows the creation of a swirl inside. This will help atomization and distribution through the exit cone.

In the Bi-Swirl, the oxidizer is normally injected into the inner swirl. When it exits, it collides with the spinning fuel from the outer swirl mixing inside the injector. This distance between both injector exits is called "Recess length" and has an impact on the injector behaviour.[38] This recess can be non-existent in some cases, where both are aligned, causing the merging of the flows inside the combustion chamber. These geometrical measurements presented in Figure 5 are attached to some ranges of variation in order to be used in Egorychev's model presented in Table 4.

4.1.1 Mixing

In bi-swirl liquid-liquid injectors, mixing happens in a recessed zone before the combustion chamber itself. In the case of using liquid fuel and oxidizer, some challenges arise in mixing. When firing with LOX-Ethanol, two separated exit

DOI: 10.13009/EUCASS2023-036

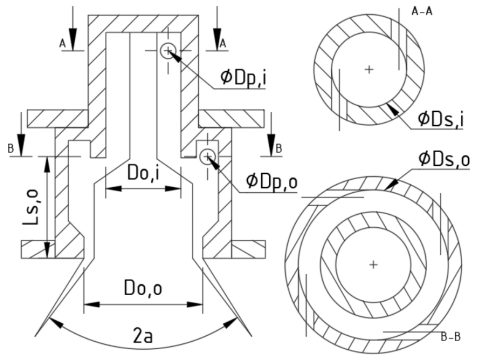

Figure 5: Bi-Swirl CAD detailing the important parameters and lengths

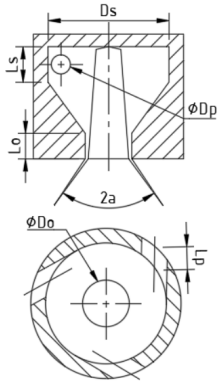

Figure 6: Simplex CAD detailing the important parameters and lengths

cones are observed instead of the single mixed cone from water tests.[8] The cause is the evaporation of oxygen during the injection. A gas oxygen layer is created and the liquids are centrifugally separated.

To solve the situation, NASA suggests using the inverse scheme, LOX used on the inside to enhance liquids mixing. This shows good performance for high-pressure cases (10-15 bar), but poor mixing in low-pressure (3-6 bar) scenarios.[8] Using large recesses "1 in" in this inverse configuration can lead to burning the injector.

Closing the gap between both "Simplex" architectures to force LOX-Ethanol impingement is not a solution as they are forced away more vigorously. The best way of achieving good mixing is by using oxygen in the outer and increasing the recess length to "1 inch" even if this would account for an average of 30% of the pressure loss in the injector.

4.1.2 Pressure Difference

In a bi-swirl, the pressure losses are normally greater than in different architectures as part of this pressure is used to make the flow swirl.

In order to estimate these losses, Egorychev's model is used.[5] This model is one of the few available that take into account the effect of the two swirl chambers to predict a result. Most of the literature available is used for single-swirl atomization. Single-swirls describe partly the behaviour that happens in the bi-swirl and can provide applicable tendencies. However, their absolute value is not useful, as the domain of application is targeted to the low mass-flow jets used in turbomachinery.

Among single-swirl correlations for the discharge coefficient, which is directly related to pressure difference by (1), we can find: Benjamin et al.,[7] Fu et al,[36] Giffen and Muraszew[6] and Rizk and Levfebre[28] among others. Since Egorychev's model is highly complex, it is difficult to study the behaviour of the injector by looking at the equations present in Annex 1. Levfebre's equation (7), is very accurate in showing each parameter's influence. It is complemented with the discharge coefficient equation (1) to obtain the correlation for pressure loss (7). The massflow ($\dot{m}$) is the total one, the area is the one of the outlet hole ($A = A_{o,o}$), and density (ρ) is the one of the mixture (ρ_e in Annex 1)

$$C_d = 0.35\left(\frac{\pi D_p^2/4}{D_s D_o}\right)^{0.5}\left(\frac{D_s}{D_o}\right)^{0.25} \qquad \Delta P = \frac{\dot{m}^2}{2\rho A^2}\cdot\left(\frac{1}{0.35}\left(\frac{D_s D_o}{\pi D_p^2/4}\right)^{0.5}\left(\frac{D_o}{D_s}\right)^{0.25}\right)^2 \tag{7}$$

From equation (7), we see the higher order term $\left(\frac{D_s D_o}{\pi D_p^2/4}\right)$ is related to the ratio of the inlet area and the chamber diameter. If the swirl chamber is increased, the swirl motion's tangential velocity will be enhanced thus causing more friction and pressure loss. Nevertheless, this parameter should be balanced as it affects jet cone angle and atomization diameter.

Ds,o (mm)	Dp(mm)	Do,o(mm)	Ds,i(mm)
13.6 ↔ 24	0.5 ↔ 2.5	$0.2D_s \leftrightarrow D_s$	$2D_p \leftrightarrow D_{s,o}$-$2D_p$-$2D_w$

Table 4: Bi-Swirl geometrical parameter operational ranges. Being Dw the wall thickness of the injector

DOI: 10.13009/EUCASS2023-036

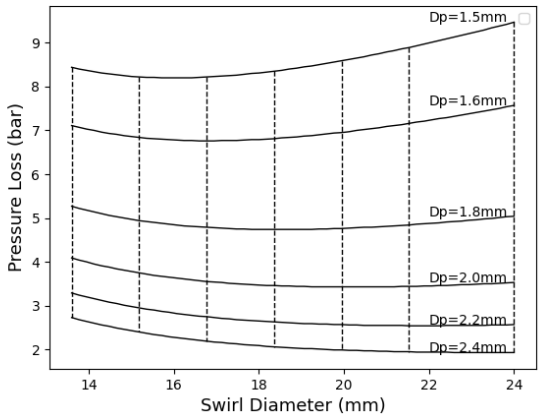

Figure 7: Pressure loss against swirl diamater "Ds,o" for different values of inlet diameter "Dp"

Parameter	Range (mm)	ΔP (bar)	Mean Drop Diameter(μm)
Ds, o	$13.77 - 24$	4.08 - 2.28	122.85 - 168.53
Dp	$0.5 - 2.4$	189.51 - 3.90	59.05 - 124.49
Do, o	$6.63 - 15.89$	4.00 - 0.91	123.99 - 224.38
Ds, i	$4.5 - 7.29$	4.00 - 4.16	124.0 - 123.18

Table 5: Tendencies for the different geometrical parameters and their variation in ΔP

The term of less importance $\left(\frac{D_o}{D_s}\right)$ is the ratio of the exit hole and the swirl diameter. When the flow comes closer to the exit hole, the friction impedes the swirl, reducing the air core. The increase in thickness and reduction in air core makes the discharge coefficient increase.[28] In Egorychev's model, these two terms are also observed. In Figure 7 we can see the influence of pressure loss with the increase of outer swirl diameter from Egorgrychev. Two different tendencies are found depending on "Dp" showing an exact coupling with the theory of the "Simplex" from Lefebvre.[28] When "Dp" is low, the effect of the first term from (7) (expressed as pressure loss) is high, showing an increase in pressure loss with the increase in swirl diameter.

When "Dp" is high, the second term becomes more relevant and the opposite effect is shown. An increase in the swirl diameter would result in a decrease in pressure drop. These effects are accentuated with the value of "Do,o" as it is multiplying in both terms. If Do is very high, only the first term would appear regardless of the value of "Dp". If Do is very low, the opposite happens. This is logical given the power of each term.

The tendencies using Egorgrychev's model for every parameter, with nominal ranges of use, are described in Table 5. These tendencies are not absolute, as there are couplings between parameters as shown in Figure 7. For calculating these tendencies, a given injector configuration was chosen and parameters were varied around this point. The configuration chosen is the one of best atomization performance at a 4 bar pressure loss. For this performance criterion, the "Do,o" should be small, thus showing in Table 5 the second term effect from Equation (7).

4.1.3 Atomization

In a bi-swirl, the atomization is normally more reliable than in different architectures, making it a good option despite the great pressure losses. In order to estimate the mean diameter at the exit, Egorychev's model is used. However, due to the complexity of the model, the single swirl models will be commented to understand the behaviour of the injector. Among correlations to find the mean drop diameter we can find: Dombrowski,[34] Jasuja,[24] Moon,[44] and Levfebre.[28] Correlation from Jasuja[24] is shown in Equation 8 as it is very accurate in showing each parameter's influence.

$$SMD = 4.4\sigma^{0.6}\nu_L^{0.16}\dot{m}_L^{0.22}(\Delta P)^{-0.43} \tag{8}$$

From Equation (8) we see the notable importance of the fuel used that will determine the kinematic viscosity (ν) and surface tension (σ). The mass flow should be fixed for each application. An increase in pressure drop would also increase the atomization, as it would increase the speed of the flow. Table 5 shows the dependencies of the geometrical parameters with the mean drop diameter. Essentially, every component follows the same trend, sizing down the injector

DOI: 10.13009/EUCASS2023-036

Mean Drop Diameter (μm)	ΔP (bar)	Ds,o (mm)	Dp(mm)	Do,o(mm)	Ds,i(mm)
123.47	4.00	15.89	2.5	5.76	5.16

Table 6: Swirl geometrical configuration with minimum drop diameter for a maximum pressure loss of 4 bar

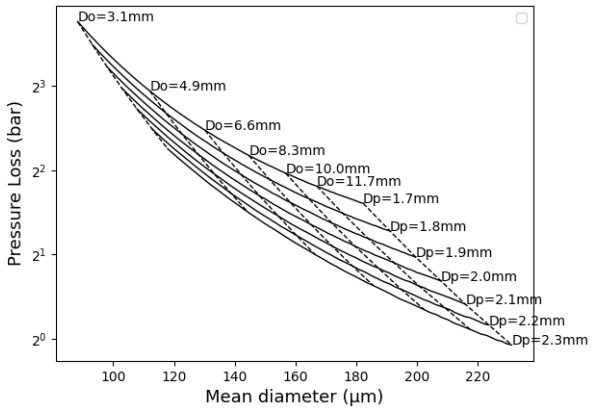

Figure 8: Pressure loss against mean drop diameter for the variation of outlet diameter "Do" and inlet diameter "Dp".

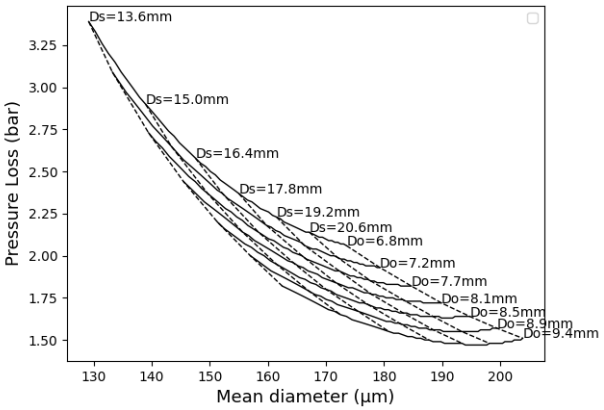

Figure 9: Pressure loss against mean drop diameter for the variation of outlet diameter "Do" and swirl diameter "Ds".

will make a smaller mean diameter. When designing the injector, it is paramount to account for the combined effect of pressure loss with atomization, as the target is to obtain a balanced design. Using Egorychev's model, the injector with the lowest mean diameter with a pressure loss between 2 bars and 4 bars was found. Its parameters are detailed in Table 6.

To understand the choice of the dimensions from Table 6, it is important to know which variables have the greatest impact on reducing the pressure loss, while not being detrimental to the drop diameter. In Figures 8 and 9 we can see how the variation of combined parameters affects the pressure loss and mean diameter. From Figure 8 the horizontal lines represent variations to "Do", while the vertical ones represent variations to "Dp". Since the slope of the vertical lines is greater, by changing "Dp", a large decrement of Δ P can be achieved without increasing the Mean diameter as much as with the "Do".

Based on the same principle, one can see in Figure 9 how it is more efficient to reduce pressure by changing "Do", than by changing "Ds". As a result of this model behaviour, the way of finding the smallest atomization for a given pressure drop consists of increasing "Dp" to the maximum specified by the range, and calculating the rest of the parameters accordingly. If less pressure drop was to be achieved after having maximized the "Dp", the "Do" should be increased before "Ds". Care should be put when increasing "Ds", as it couples with "Do" and "Dp" and a minimum pressure loss is found, as seen in Figure 9. This would mean that increasing "Ds" can increase the pressure drop while increasing the mean drop diameter, which is not desirable.

4.1.4 Instabilities

The main instability types acting on the Bi-swirl are "Chugg" and "High frequency". "Self pulsation" oscillatory behaviour can also appear. These conclusions were obtained from the Ethanol-LOX 15kN NASA engine.[8] Chugg instabilities can happen due to bubbles in the LOX or during the start-up. This may be caused by the low pressure as they disappear when reaching steady operation (3-9 bar). High-frequency instabilities are shown in very high-pressure (above 20 bar). Oscillations are coupled with the chamber's natural frequency with a magnitude of 2 bar for this case.

5. Shear Coaxial

The shear coaxial injector is a widely used configuration in many prominent LREs (Liquid Rocket Engines), such as the SSME (Space Shuttle Main Engine). It has simple yet effective operating premise and can be easily manufactured. Coaxial elements can deliver good atomisation, low pressure drop, and good wall compatibility. However, there are

DOI: 10.13009/EUCASS2023-036

some challenges with the mixing and manufacturing tolerances for very small annulus gaps. Care should also be taken to address instabilities in throttable engine applications. It is primarily encountered in gas-liquid applications, so this research is largely an effort to determine whether its results can be extrapolated to biliquid configurations.

5.1 Injection Elements & Geometrical Considerations

In this injector design, the propellants flow concentrically, with the liquid at a higher rate in the inner annulus, and the gas at a faster one on the outer profile. The velocity difference creates a shearing effect that atomises the liquid jet. Figure 10 demonstrates the key geometrical considerations of the design. Firstly, the diameter of the fuel and oxidiser respectively can be identified. Furthermore, the recess length of the inner tube is also crucial, as it corresponds to the impingement length in other injectors. This parameter represents the difference in distance between the two propellants, indicating the zone of mixing before entering the combustion chamber. Finally, the thickness and length of the injector post (i.e. the inner concentric tube) are significant for the structural integrity of the injector, as well as the prevention of instabilities.

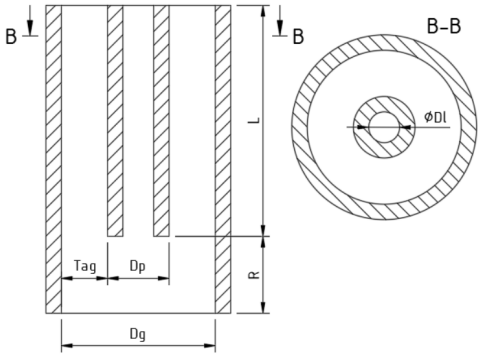

Figure 10: Shear injector section CAD with the main geometrical dimensions

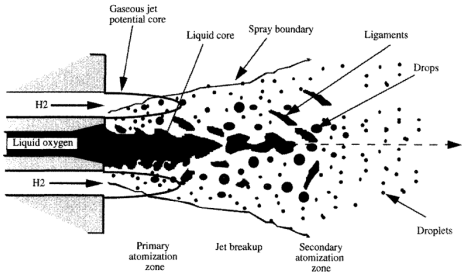

Figure 11: Shear injector atomisation

5.1.1 Pressure Difference

From the experience obtained through several injector test campaigns over the years, the rule of thumb developed is that the pressure drop across the injector is some percentage of the chamber pressure. Typically, it is of the order 20-25%. However, the figure can vary based on the injector type. Coaxial injectors (i.e. the concentric tube configuration) has even recorded far lower bounds of about 5%.[18]

Regarding the parameters that most influence pressure losses in coaxial shear injectors, the primary one is the recess length. Notably, Lux and Haidn[32] studied the effect of a recessed LOX tube for a LOX-methane configuration. They found that at a low momentum flux ratio, the pressure drop across the injector increases with a recessed liquid oxygen tube when compared with a flush tube. Furthermore, the geometry of the orifice plays a significant part in terms of exit velocity and subsequent pressure drop.

During the review of empirical correlations for coaxial shear injector performance, no such equations were found to estimate the pressure loss or discharge coefficient that were specific to this type of injector. Therefore Equation 9 (left) was used to estimate the pressure losses for each propellant. The equation depends on the propellant's density, velocity, and head loss coefficient, K. This parameter accounts for irreversible pressure losses. Its value is given as 1.2 for radiused (rounded inlets) and 1.7 for sharp (chamfered) ones.[18] It is worth highlighting that given the density differences between the outer jet (gas) and the inner (liquid), at nominal air/liquid ratios, the pressure drop in the gas tube will be considerably higher than in the liquid one. The value obtained can be then substituted into the traditional Cd equation to estimate the coefficient of discharge for each of the tubes.

5.1.2 Atomization

The atomisation in the shear is highly dependent on the exit orifice, the fluid velocity and the propellant properties. This can be verified in several correlations that used this injector for different applications including rocket propulsion, turbomachinery and RAM jets, as seen in Table 7

DOI: 10.13009/EUCASS2023-036

Reference	Measure	Experimental conditions
Lorenzetto & Lefebvre 1977[30]	d_{32}	Water/Kerosene $0.001 \leq \mu \leq 0.076$ kg/ms, liquid surface tension: $0.026 \leq \sigma \leq 0.076$ N/m, liquid density: $794 \leq \rho \leq 2,180$ kg/m^3, air velocity: $70 \leq V \leq 180$ m/s, air/liquid mass ratio: 1-16
Ingebo 1989[20]	d_{32}	$0.32 \leq d_0 \leq 0.56$, Atomizing gas mass flux ranged from 6 to 50 $\frac{g}{cm^2 sec}$, gas molecular weight range of 4 to 44
Zaller 1991[47]	d_{32}	Water flow rate: 0.0032 kg/s, air flow rates: 0.0027, 0.0041, & 0.0055 kg/s
Weiss & Worsham 1959[43]	$d_{v0.5}$	Dyed wax at Temperature: (300, 350, 400) F, specific gravity: [0.828, 0.811, 0.806], Surface Tension: (22.0, 20.1 18.2) dyne/cm, Viscosity: (11.3, 5.86, 3.25) centipoise
Kim & Marshall 1971[25]	$d_{v0.5}$	Mass flow ratio: 0.06-40, Relative velocity: 250 ft./sec. to sonic velocity, Viscosity: 1-50 cp

Table 7: Coaxial Shear Injector Correlations

Ingebo's SMD correlation[21] was selected to test whether this injector is applicable to the MINERVA engine. It was deemed suitable as it was tested for rocket propulsion, used similar propellants, and fit our operating range as detailed in Table 8. The equation itself is described in Equation 9 (right).
Table 9 provides a comparison between the parameters of LN_2, used in Ingebo's experiment, and Ethanol, used in the MINERVA, to check the similarity of both liquids and applicability of the correlations. The data from Ethanol was chosen to carry out all the calculations. An arbitrary mass flow of 2kg/s with a number of 61 injectors was used to match the order of magnitude of the Minerva.

D_l **(mm)**	D_g **(mm)**	**air-liquid ratio**	$\dot{m}_l$ **(g/s)**	$\dot{m}_g$ **(g/s)**
2.95 - 5.64	3.6 - 6.6	0.2 - 0.625	27	6 - 17

Table 8: Ranges of operation for relevant geometrical and sizing parameters

Fluid	**density** (kg/m^3)	**Surface tension** (mN/m)	**viscosity** $(mPa \cdot s)$
LN2	806	8.9	0.1
Ethanol	789	22.0	0.98

Table 9: Comparison between Liquid nitrogen and ethanol characteristics

$$\Delta P = K\frac{1}{2}\rho v^2; \qquad \frac{D_g}{SMD} = 8.1\left(\frac{\rho_g^2 D_g^2 W_g^2}{\mu_l \sigma_l \rho_l}\right)^{0.44} \tag{9}$$

The parameters influencing atomization are also dependent on the mass flow. A higher mass flow at a constant diameter will require more pressure and will provide better atomization. When changing the air/liquid ratio, even if the rocket mass flow is kept, the mass flow of each propellant changes, obtaining Figure 12.
In Figure 12, several curves are obtained by varying the exit air diameter "Dg" across its nominal range, for three different gas/liquid ratios. It can be seen that both variables reduce the pressure drop similarly, as the curves almost merge. But changing the ratio allows elongating the curve across other drop diameter values, which could not be achievable within the nominal "Dg" range and a fixed ratio.
One of the advantages of shear injectors is the small size, compared to other injectors like the swirl. As such, a higher number of them can be used, thus obtaining a very homogeneous flow to prevent instabilities. In Figure 13, the diameter of the gas exit diameter "Dg" was changed in the nominal range, while keeping the gas/liquid ratio fixed at 1/5. As the "Dg" becomes bigger, a configuration with fewer injectors is chosen to fit the 0.1 m diameter combustion chamber. The three resultant injector configurations are the three lines represented in the figure. Each line shows the pressure loss and drop size change when varying the "Dg" in a given injector packing. When the "Dg" diameter is very small (dotted line), the number of injectors is high, decreasing the mass flow per injector, reducing the pressure loss, and obtaining good atomization because of its small size. Further increasing the diameter, forces to reduce the number of injectors

DOI: 10.13009/EUCASS2023-036

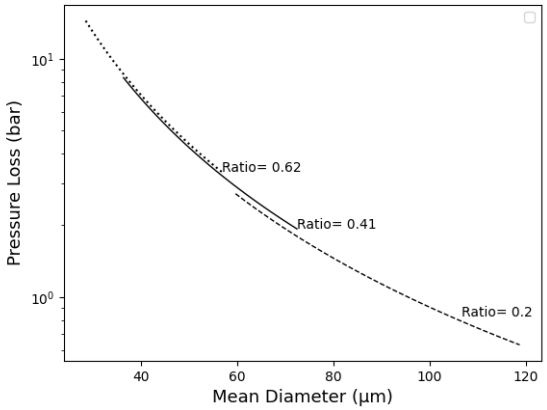

Figure 12: Pressure loss against drop mean diameter for a change in "Dg" and in air/liquid ratio

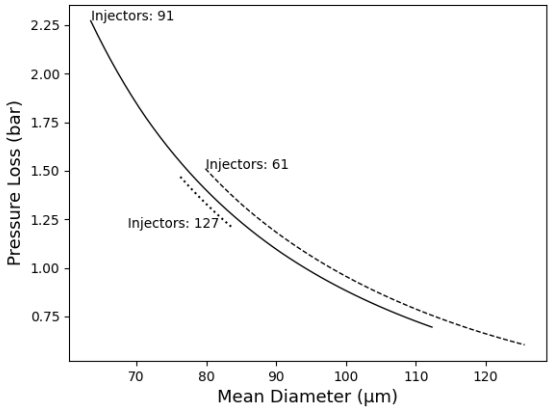

Figure 13: Pressure loss against drop mean diameter for a change in "Dg" that results in a change in injector number

(plain and dashed lines) and increase the mass flow per injector. Increasing the mass flow will increase the velocity, decreasing the drop size and increasing the pressure drop.
The most efficient diameter is the one that allows dense packing inside the chamber. Increasing the number of injectors permits us to have a smaller drop size for a given pressure drop.

5.1.3 Mixing

Mixing in a shear injector is mainly defined by three parameters: Mixing Ratio, the Coaxial parameter and the Velocity Head Ratio. The mixture ratio describes the injection ratio (mass flow rate ratio) of the fuel to the oxidiser. It has a direct impact on the stability and durability of the combustion chamber. Furthermore, coupled with the recess length of the injector, it can affect droplet size and mixing uniformity. The coaxial parameter (Cp), given by Equation (10), was proposed by Falk and Nurick in an attempt to produce an optimising expression for the gas-liquid coaxial injector, after finding that increasing the gaseous velocity can improve the mixing. The velocity head ratio (VHR) is akin to the ΔP ratio. It is generally advised to have values as close to 1 as possible. It is shown in Equation (10).

$$Cp = \frac{(\rho_g V_g)^2}{MRV_l}; \quad VHR = \frac{\rho_{fuel}}{\rho_{oxidiser}} \left(\frac{A_{fuel}\dot{m}_{fuel}}{A_{oxidiser}\dot{m}_{oxidiser}}\right)^2 \tag{10}$$

5.1.4 Instabilities

Instability analysis in coaxial shear injectors is particularly interesting, as we can distinguish between favourable and unfavourable ones. Atomisation in this type of injector occurs thanks to surface instabilities which lead to jet break-up and the formation of droplets. However, unstable pressure oscillations may occur within the chamber, when there is a strong coupling between atomisation, vaporisation, and burning. Instabilities in the coaxial injector are highly dependent on the velocity ratio, the recess length (it is custom to recess the oxidiser post, to increase combustion efficiency and stability against high-frequency fluctuations.[11]), as well as geometrical parameters such as chamfering or tapering of the tubes.

6. Minerva Engine Approach

The aim of this project at Perseus is to present a version of the injection system that can outperform the current one. After studying the different types and configurations, each injector has its own strengths and weaknesses.

The impinging shows somewhat similar ΔP- Drop diameter ratio in theory compared to the other types but is very sensitive to manufacturing imperfections that can ruin performance. This injector remains simple to design and was a good initial choice for the MINERVA.The bi-swirl is very robust in terms of manufacturing precision but contains more elements adding complexity. The behaviour of the injector is very well understood to sort out the complexity and benefit for the reliable operation of this injector. Even if the performance is not dramatically better than the impinging, it is enough to burn the majority of fuel before exiting the chamber with a relatively low pressure drop. Finally, the shear is operated with gas and liquid, meaning the oxygen should be gas before entering the injector. The configuration

DOI: 10.13009/EUCASS2023-036

presented is heavily oriented to nitrogen gas, but its properties are very different from oxygen. The correlations found are the closest available to the Minerva, but may still not apply as they are not meant to be used in this context. However, they show a similar performance as the impinging, without the tight manufacturing constraints. As such, is worth to further explore the shear coaxial configuration and its applications to a biliquid test case.

7. Conclusion

The work done in this paper depict the impact of geometric design variables on the performance of three types LPRE injectors; impinging, shear and swirl. It is clear to see that slight changes in the sizing have considerable influence on atomization and pressure drop. The sizing of an injector is composed of a qualitative part: good practices outlined for each injector and quantitative considerations. The set of equations described for each injector and range of operation have been gathered into a Python widget sizing tool. This tool is a compilation of all correlations presented so that the user can estimate expected injector performance with geometrical inputs, propellants and constraints. The paper and the tool are complementary to designing an injector. The tool would allow for predicting performance, but the article indicates which parameters trigger the desired effect on the results.

8. Acknowledgments

The authors would like to thank the passionate team of supervisors overseeing the propulsion projects of PERSEUS. Particularly we thank Jean-Noël Chopinet (Engineer, previously at ArianeGroup, Vernon), Annafederica Urbano (Research Engineer and Professor at ISAE-Supaéro) and Jean-Philippe Joubert (Engineer at Arianegroupe, Vernon). We also thank Elouan Maître and Niels Albrecht for their involvement in the siwrl injector mechanical design.

References

[1] G. Bailardi. On the atomization behavior of newtonian fluids with an impinging jet injector. 2010.
[2] Vladimir Bazarov. Liquid rocket thrust chambers : aspects of modeling, analysis, and design. 2004.
[3] R. Dickerson, K. Tate, and N. Barsic. Correlation of spray injector parameters with rocket engine performance. Technical Report R-7499 AFRPL-TR-68-147, Rocketdyne, June 1968.
[4] N. Dombrowski Dombrowski and P. C. Hooper. A study of the sprays formed by impinging jets in laminar and turbulent flow. *Journal of Fluid Mechanics*, 18(3):392–400, March 1964. Publisher: Cambridge University Press.
[5] V.S. Egoryhev. *Calculation and Design of Mixing in Liquid Rocket Engines*. Samara Publishing house SGAU, Samara State Aerospace University, under the Ministry of Education and Science of the Russian Federation, 2011. Translated by the authors from Russian using as reference the work of Vladimir Bazarov in Chapter 2 of Bazarov 2004, Design and Dynamics of Jet and Swirl Injectors.
[6] J. Xue et al. Effect of geometric parameters on simplex atomizer performance, December 2004.
[7] M. A. Benjamine et al. Film thickness, droplet size measurements and correlations for large pressure-swirl atomizers, June 1998.
[8] R.D. Woodward et al. Injector research for shuttle qms upgrade using lox/ethanol propellants, August 2012. 34th AIAA/ASME/SAE/ASEE Joint Propulsion Conference and Exhibit.
[9] S.Soller et al. Combustion stability characteristics of coax-swirl-injectors for oxygen/kerosene july 2007, July 2007. Conference: 43rd AIAA/ASME/SAE/ASEE Joint Propulsion Conference Exhibit.
[10] Y. Chelkis et al. Incorporation of rd-180 failure response features in the atlas v booster emergency detection system, 2011.
[11] Y. Nunome et al. Effect of liquid disintegration on flow instability in a recessed region of a shear coaxial injector. In *45th AIAA/ASME/SAE/ASEE Joint Propulsion Conference Exhibit*. AIAA, August 2009.
[12] A. Ferrenberg, K. Hunt, and J. Duesberg. Atomization and Mixing Study. Technical Report NAS 1.26:178751, December 1985.
[13] Youngquist R. Friant D.R., Kircher H.J. Discharge coefficient for common orifice forms. Technical report, Reaction Motors, Inc., February 1954.
[14] D. GEORGE. Rocket injector hot firing and cold flow spray fields. In *9th Propulsion Conference*. AIAA, August 1973.
[15] G. S. Gill and W. H. Nurick. Liquid rocket engine injectors, March 1976.
[16] Sanford Gordon and Bonnie J. Mcbride. Computer program for calculation of complex chemical equilibrium compositions and applications. Part 1: Analysis, October 1994.
[17] Donald Hautman. Spray characterization of like-on-like doublet impinging rocket injectors. *AIAA*, 1991.

DOI: 10.13009/EUCASS2023-036

[18] David H. Huang and Dieter K. Huzel. *Modern Engineering for Design of Liquid-Propellant Rocket Engines*. AIAA, January 1992.

[19] I.Petkov S. Bletch I. Muller, M. Kuhn. 3d-printed coaxial fuel injector for a lox/kerosene rocket engine, May 2018. Conference: Space Propulsion 2018.

[20] R. Ingebo. Dropsize correlation for cryogenic liquid-jet atomization. NASA Technical Memorandum 2751, National Aeronautics and Space Administration, 1991.

[21] Robert D. Ingebo. Drop-size Distributions for Impinging-jet Breakup in Airstreams Simulating the Velocity Conditions in Rocket Combustors, March 1958.

[22] Chihiro INOUE, Yuta TAKEUCHI, Koji NOZAKI, Takehiro HIMENO, Toshinori WATANABE, Go FUJII, and Yu DAIMON. Unified length scale of spray structure by unlike impinging jets. *TRANSACTIONS OF THE JAPAN SOCIETY FOR AERONAUTICAL AND SPACE SCIENCES*, 62(4):213–218, 2019.

[23] Jackson I. Ito. Propellant injection systems and processes. Technical report, January 1995.

[24] A. K. Jasuja. Atomization of crude and residual fuel oils, April 1979.

[25] K. Y. Kim and W. R. Marshall. Drop-size distributions from pneumatic atomizers. *AIChE Journal*, 17(3):575–584, May 1971.

[26] Kenneth Kuan-Yun Kuo. *Principles of Combustion*. John Wiley & Sons, Nashville, TN, 2 edition, January 2005.

[27] Wei-Hsiang Lai, Tzu-Hong Huang, Tsung-Leo Jiang, and Wennon Huang. Effects of fluid properties on the characteristics of impinging jet sprays. *Atomization and Sprays*, 15(4):457–468, 2005.

[28] Arthur Lefebvre and Vincent Mcdonell. *Atomization and Sprays, Second Edition*. April 2017.

[29] Byoung-Jik Lim, Ki-Hoon Jung, Tae-Ock Khil, and Young-Bin Yoon. Effect of ambient gas density and injection velocity on the atomization characteristics of impinging jet. *Journal of the Korean Society for Aeronautical & Space Sciences*, 32, August 2004.

[30] G. E. Lorenzetto and A. H. Lefebvre. Measurements of drop size on a plain-jet airblast atomizer. *AIAA Journal*, 15(7):1006–1010, July 1977.

[31] D. Lourme. Like-on-like injection spray characterization for the Ariane Viking engine. In *22nd Joint Propulsion Conference*, Joint Propulsion Conferences. AIAA, June 1986.

[32] Johannes Lux and Oskar Haidn. Effect of recess in high-pressure liquid oxygen/methane coaxial injection and combustion. *Journal of Propulsion and Power*, 25(1):24–32, January 2009.

[33] P. Veres M. Binder, T. Tomsik. Rl10a-3-3a rocket engine modeling project, January 1997. NASA Technical Reports Server.

[34] P.C. Hooper N. Dombrowski. The effect of ambient density on drop formation in sprays, April 1961.

[35] W. H. Nurick. Orifice Cavitation and Its Effect on Spray Mixing. *Journal of Fluids Engineering*, 98(4):681–687, 12 1976.

[36] W. Zhang Q.Fu, L.Yang. Spray characteristics of an open-end swirl injector, January 2012.

[37] H. M. Ryan, W. E. Anderson, S. Pal, and R. J. Santoro. Atomization characteristics of impinging liquid jets. *Journal of Propulsion and Power*, 11(1):135–145, January 1995. Publisher: AIAA.

[38] Y.Yoon S.Kim, J.Yoon. Internal flow characteristics of liquid-liquid swirl coaxial injectors with different recess lengths and oxidizer-fuel ratios, January 2011.

[39] Bimal Subedi, Min Son, Woojin Kim, Jangsu Choi, and Jaye Koo. Spray characteristics of misaligned impinging injectors. *Journal of the Korean Society of Marine Engineering*, 38(10):1257–1262, December 2014.

[40] George P. Sutton. *History of liquid propellant rocket engines*. AIAA, Reston, Virginia, 2006.

[41] George Paul Sutton and Oscar Biblarz. *Rocket propulsion elements*. John Wiley & Sons, Hoboken, N.J., 8th ed edition, 2010.

[42] Brian A. Sweeney and Robert A. Frederick. Jet breakup length to impingement distance ratio for like doublet injectors. *Journal of Propulsion and Power*, 32(6):1516–1530, November 2016.

[43] MALCOLM A. WEISS and CHARLES H. WORSHAM. Atomization in high velocity airstreams. *ARS Journal*, 29(4):252–259, April 1959.

[44] Y. Yoon Y.Moon, D.Kim. Atomization of crude and residual fuel oils, April 2010.

[45] L. J. Zajac. Correlation of spray dropsize distribution and injector variables. Technical Report R-7995, January 1971.

[46] L. J. Zajac. Droplet breakup in accelerating gas flows. Part 2: Secondary atomization. Technical Report NASA-CR-134479, October 1973.

[47] M. Zaller. Lox/hydrogen coaxial injector atomisation test program. NASA Contractor Report 187037, National Aeronautics and Space Administration, 1990.

DOI: 10.13009/EUCASS2023-036

Appendices

A. Egorychev's model

Model described in the Swirl injector section. Set of equations needed to calculate the performance in mean diameter drop size, cone angle and discharge coefficient from propellants characteristics and geometrical features.

Where e is the ratio of the density of the oxidizer and fuel, K_m is the mixing ratio oxidizer to fuel, and η_F and η_O are the dynamic viscosities of fuel and oxidizer. Letter i, o represents the number of inlet holes in the outlet chamber. ρ represented density (Being ρ_k the density of the products.) and σ represents surface tension. Parameters A_{em} and $A_{e,em}$ are intermediate steps to calculate φ, the relationship between the diameter of the air (D_{air}) core and exit. The calculated discharge coefficient is represented by μ. The angle of the exit cone is two times α. Uppercase $A_{o,o}$ references the area of outlet, being $W_{a,e}$ the speed of the flow at the exit. Parameter d_M, mean drop diameter is highly dependant on L_p, very related to δ_n, the thickness of the film.

$$\eta_e = \frac{\eta_F + K_m \eta_O}{1 + K_m} \tag{11}$$

$$D_{pk} = Dp\sqrt{i, o} \tag{12}$$

$$Re = \frac{4mf}{\pi \eta_e D_{pk}} \tag{13}$$

$$\rho_e = \frac{e\rho_F(1 + K_m)}{K_m + e} \tag{14}$$

$$\log \lambda = \frac{25.8}{(\log Re)^{2.58}} - 2 \tag{15}$$

$$A_{em} = \frac{\left(K_m \frac{R_{s,i}}{R_{s,o}} + \sqrt{e}\right)\sqrt{e}}{(1 + K_m)(K_m + e)} \frac{R_{s,o} R_{o,o}}{i, R_p^2} \tag{16}$$

$$A_{e,em} = \frac{A_{em}}{1 + \frac{\lambda}{2} A_{em}\left(\frac{(R_{s,o}+R_p)^2+R_p}{r_{o,o}^2} - 1\right)} \tag{17}$$

$$\varphi = 1 - \frac{D_{air}^2}{D_{o,o}^2} = \frac{1}{\left(\sqrt[3]{\frac{A_{e,em}}{2\sqrt{2}} + \sqrt{\frac{A_{e,em}^2}{8} - \frac{1}{27}}} + \sqrt[3]{\frac{A_{e,em}}{2\sqrt{2}} - \sqrt{\frac{A_{e,em}^2}{8} - \frac{1}{27}}}.\right)^2} \tag{18}$$

$$\mu = \varphi\sqrt{\frac{\varphi}{2 - \varphi}} \tag{19}$$

$$\tan \alpha = \frac{2\mu A_{e,em}}{\sqrt{(1 + \sqrt{1 - \varphi})^2 - 4\mu^2 A_{e,em}^2}} \tag{20}$$

$$W_{a,e} = \frac{mf}{\rho_e A_{o,o}} \qquad W_e = \frac{W_{a,e}}{\cos \alpha} \tag{21}$$

$$We = \frac{\rho_k W_e^2 D_{o,o}}{\sigma_e} \tag{22}$$

$$\delta_n = R_{o,o} - R_{air} \qquad R_{air} = R_{o,o}\sqrt{1 - \varphi} \tag{23}$$

$$L_p = \frac{\rho_e \delta_n \sigma_e}{\eta_e} \tag{24}$$

$$d_M = 269 L_p^{-0.35}\left(\frac{We\rho_k}{\rho_e}\right)^{-0.483} \tag{25}$$

The text advises to use the following ranges of relative dimensions in swirl injector design: D_o/D_s = 0.2-1.0, L_o/D_o = 0.2-1.0 and D_s/L_s = 0.5-3.0.